

Precise measurement of the top quark mass from lepton+jets events

- V.M. Abazov³⁶, B. Abbott⁷⁵, M. Abolins⁶⁵, B.S. Acharya²⁹, M. Adams⁵¹, T. Adams⁴⁹, E. Aguilo⁶, M. Ahsan⁵⁹, G.D. Alexeev³⁶, G. Alkhazov⁴⁰, A. Alton^{64,a}, G. Alverson⁶³, G.A. Alves², M. Anastasoaie³⁵, L.S. Ancu³⁵, T. Andeen⁵³, B. Andrieu¹⁷, M.S. Anzelc⁵³, M. Aoki⁵⁰, Y. Arnoud¹⁴, M. Arov⁶⁰, M. Arthaud¹⁸, A. Askew⁴⁹, B. Åsman⁴¹, A.C.S. Assis Jesus³, O. Atramentov⁴⁹, C. Avila⁸, F. Badaud¹³, L. Bagby⁵⁰, B. Baldin⁵⁰, D.V. Bandurin⁵⁹, P. Banerjee²⁹, S. Banerjee²⁹, E. Barberis⁶³, A.-F. Barfuss¹⁵, P. Bargassa⁸⁰, P. Baringer⁵⁸, J. Barreto², J.F. Bartlett⁵⁰, U. Bassler¹⁸, D. Bauer⁴³, S. Beale⁶, A. Bean⁵⁸, M. Begalli³, M. Begel⁷³, C. Belanger-Champagne⁴¹, L. Bellantoni⁵⁰, A. Bellavance⁵⁰, J.A. Benitez⁶⁵, S.B. Beri²⁷, G. Bernardi¹⁷, R. Bernhard²³, I. Bertram⁴², M. Besançon¹⁸, R. Beuselinck⁴³, V.A. Bezzubov³⁹, P.C. Bhat⁵⁰, V. Bhatnagar²⁷, C. Biscarat²⁰, G. Blazey⁵², F. Blekman⁴³, S. Blessing⁴⁹, D. Bloch¹⁹, K. Bloom⁶⁷, A. Boehlein⁵⁰, D. Boline⁶², T.A. Bolton⁵⁹, E.E. Boos³⁸, G. Borissov⁴², T. Bose⁷⁷, A. Brandt⁷⁸, R. Brock⁶⁵, G. Brooijmans⁷⁰, A. Bross⁵⁰, D. Brown⁸¹, X.B. Bu⁷, N.J. Buchanan⁴⁹, D. Buchholz⁵³, M. Buehler⁸¹, V. Buescher²², V. Bunichev³⁸, S. Burdin^{42,b}, T.H. Burnett⁸², C.P. Buszello⁴³, J.M. Butler⁶², P. Calfayan²⁵, S. Calvet¹⁶, J. Cammin⁷¹, E. Carrera⁴⁹, W. Carvalho³, B.C.K. Casey⁵⁰, H. Castilla-Valdez³³, S. Chakrabarti¹⁸, D. Chakraborty⁵², K.M. Chan⁵⁵, A. Chandra⁴⁸, E. Cheu⁴⁵, F. Chevallier¹⁴, D.K. Cho⁶², S. Choi³², B. Choudhary²⁸, L. Christofek⁷⁷, T. Christoudias⁴³, S. Cihangir⁵⁰, D. Claes⁶⁷, J. Clutter⁵⁸, M. Cooke⁵⁰, W.E. Cooper⁵⁰, M. Corcoran⁸⁰, F. Couderc¹⁸, M.-C. Cousinou¹⁵, S. Crépé-Renaudin¹⁴, V. Cuplov⁵⁹, D. Cutts⁷⁷, M. Ćwiok³⁰, H. da Motta², A. Das⁴⁵, G. Davies⁴³, K. De⁷⁸, S.J. de Jong³⁵, E. De La Cruz-Burelo⁶⁴, C. De Oliveira Martins³, J.D. Degenhardt⁶⁴, F. Déliot¹⁸, M. Demarteau⁵⁰, R. Demina⁷¹, D. Denisov⁵⁰, S.P. Denisov³⁹, S. Desai⁵⁰, H.T. Diehl⁵⁰, M. Diesburg⁵⁰, A. Dominguez⁶⁷, H. Dong⁷², T. Dorland⁸², A. Dubey²⁸, L.V. Dudko³⁸, L. Duflot¹⁶, S.R. Dugad²⁹, D. Duggan⁴⁹, A. Duperrin¹⁵, J. Dyer⁶⁵, A. Dyshkant⁵², M. Eads⁶⁷, D. Edmunds⁶⁵, J. Ellison⁴⁸, V.D. Elvira⁵⁰, Y. Enari⁷⁷, S. Eno⁶¹, P. Ermolov^{38,‡}, H. Evans⁵⁴, A. Evdokimov⁷³, V.N. Evdokimov³⁹, A.V. Ferapontov⁵⁹, T. Ferbel⁷¹, F. Fiedler²⁴, F. Filthaut³⁵, W. Fisher⁵⁰, H.E. Fisk⁵⁰, M. Fortner⁵², H. Fox⁴², S. Fu⁵⁰, S. Fuess⁵⁰, T. Gadfort⁷⁰, C.F. Galea³⁵, C. Garcia⁷¹, A. Garcia-Bellido⁸², V. Gavrilov³⁷, P. Gay¹³, W. Geist¹⁹, D. Gelé¹⁹, W. Geng^{15,65}, C.E. Gerber⁵¹, Y. Gershtein⁴⁹, D. Gillberg⁶, G. Ginther⁷¹, N. Gollub⁴¹, B. Gómez⁸, A. Goussiou⁸², P.D. Grannis⁷², H. Greenlee⁵⁰, Z.D. Greenwood⁶⁰, E.M. Gregores⁴, G. Grenier²⁰, Ph. Gris¹³, J.-F. Grivaz¹⁶, A. Grohsjean²⁵, S. Grünenwald⁵⁰, M.W. Grünewald³⁰, F. Guo⁷², J. Guo⁷², G. Gutierrez⁵⁰, P. Gutierrez⁷⁵, A. Haas⁷⁰, N.J. Hadley⁶¹, P. Haefner²⁵, S. Hagopian⁴⁹, J. Haley⁶⁸, I. Hall⁶⁵, R.E. Hall⁴⁷, L. Han⁷, K. Harder⁴⁴, A. Harel⁷¹, J.M. Hauptman⁵⁷, R. Hauser⁶⁵, J. Hays⁴³, T. Hebbeker²¹, D. Hedin⁵², J.G. Hegeman³⁴, A.P. Heinson⁴⁸, U. Heintz⁶², C. Hensel^{22,d}, K. Herner⁷², G. Hesketh⁶³, M.D. Hildreth⁵⁵, R. Hirosky⁸¹, J.D. Hobbs⁷², B. Hoeneisen¹², H. Hoeth²⁶, M. Hohlfeld²², S. Hossain⁷⁵, P. Houben³⁴, Y. Hu⁷², Z. Hubacek¹⁰, V. Hynek⁹, I. Iashvili⁶⁹, R. Illingworth⁵⁰, A.S. Ito⁵⁰, S. Jabeen⁶², M. Jaffré¹⁶, S. Jain⁷⁵, K. Jakobs²³, C. Jarvis⁶¹, R. Jesik⁴³, K. Johns⁴⁵, C. Johnson⁷⁰, M. Johnson⁵⁰, A. Jonckheere⁵⁰, P. Jonsson⁴³, A. Juste⁵⁰, E. Kajfasz¹⁵, J.M. Kalk⁶⁰, D. Karmanov³⁸, P.A. Kasper⁵⁰, I. Katsanos⁷⁰, D. Kau⁴⁹, V. Kaushik⁷⁸, R. Kehoe⁷⁹, S. Kermiche¹⁵, N. Khalatyan⁵⁰, A. Khanov⁷⁶, A. Kharchilava⁶⁹, Y.M. Kharzeev³⁶, D. Khatidze⁷⁰, T.J. Kim³¹, M.H. Kirby⁵³, M. Kirsch²¹, B. Klíma⁵⁰, J.M. Kohli²⁷, J.-P. Konrath²³, A.V. Kozelov³⁹, J. Kraus⁶⁵, T. Kuhl²⁴, A. Kumar⁶⁹, A. Kupco¹¹, T. Kurča²⁰, V.A. Kuzmin³⁸, J. Kvita⁹, F. Lacroix¹³, D. Lam⁵⁵, S. Lammers⁷⁰, G. Landsberg⁷⁷, P. Lebrun²⁰, W.M. Lee⁵⁰, A. Leflat³⁸, J. Lellouch¹⁷, J. Li^{78,‡}, L. Li⁴⁸, Q.Z. Li⁵⁰, S.M. Lietti⁵, J.K. Lim³¹, J.G.R. Lima⁵², D. Lincoln⁵⁰, J. Linnemann⁶⁵, V.V. Lipaev³⁹, R. Lipton⁵⁰, Y. Liu⁷, Z. Liu⁶, A. Lobodenko⁴⁰, M. Lokajicek¹¹, P. Love⁴², H.J. Lubatti⁸², R. Luna³, A.L. Lyon⁵⁰, A.K.A. Maciel², D. Mackin⁸⁰, R.J. Madaras⁴⁶, P. Mättig²⁶, C. Magass²¹, A. Magerkurth⁶⁴, P.K. Mal⁸², H.B. Malbouisson³, S. Malik⁶⁷, V.L. Malyshev³⁶, H.S. Mao⁵⁰, Y. Maravin⁵⁹, B. Martin¹⁴, R. McCarthy⁷², A. Melnitchouk⁶⁶, L. Mendoza⁸, P.G. Mercadante⁵, M. Merkin³⁸, K.W. Merritt⁵⁰, A. Meyer²¹, J. Meyer^{22,d}, T. Millet²⁰, J. Mitrevski⁷⁰, R.K. Mommesen⁴⁴, N.K. Mondal²⁹, R.W. Moore⁶, T. Moulik⁵⁸, G.S. Muanza²⁰, M. Mulhearn⁷⁰, O. Mundal²², L. Mundim³, E. Nagy¹⁵, M. Naimuddin⁵⁰, M. Narain⁷⁷, N.A. Naumann³⁵, H.A. Neal⁶⁴, J.P. Negret⁸, P. Neustroev⁴⁰, H. Nilsen²³, H. Nogima³, S.F. Novaes⁵, T. Nunnemann²⁵, V. O'Dell⁵⁰, D.C. O'Neil⁶, G. Obrant⁴⁰, C. Ochando¹⁶, D. Onoprienko⁵⁹, N. Oshima⁵⁰, N. Osman⁴³, J. Osta⁵⁵, R. Otec¹⁰, G.J. Otero y Garzón⁵⁰, M. Owen⁴⁴, P. Padley⁸⁰, M. Pangilinan⁷⁷, N. Parashar⁵⁶, S.-J. Park^{22,d}, S.K. Park³¹, J. Parsons⁷⁰, R. Partridge⁷⁷, N. Parua⁵⁴, A. Patwa⁷³, G. Pawloski⁸⁰, B. Penning²³, M. Perfilov³⁸, K. Peters⁴⁴, Y. Peters²⁶, P. Pétroff¹⁶, M. Petteni⁴³, R. Piegaia¹, J. Piper⁶⁵, M.-A. Pleier²², P.L.M. Podesta-Lerma^{33,c},

V.M. Podstavkov⁵⁰, Y. Pogorelov⁵⁵, M.-E. Pol², P. Polozov³⁷, B.G. Pope⁶⁵, A.V. Popov³⁹, C. Potter⁶, W.L. Prado da Silva³, H.B. Prosper⁴⁹, S. Protopopescu⁷³, J. Qian⁶⁴, A. Quadt^{22,d}, B. Quinn⁶⁶, A. Rakitine⁴², M.S. Rangel², K. Ranjan²⁸, P.N. Ratoff⁴², P. Renkel⁷⁹, S. Reucroft⁶³, P. Rich⁴⁴, J. Rieger⁵⁴, M. Rijssenbeek⁷², I. Ripp-Baudot¹⁹, F. Rizatdinova⁷⁶, S. Robinson⁴³, R.F. Rodrigues³, M. Rominsky⁷⁵, C. Royon¹⁸, P. Rubinov⁵⁰, R. Ruchti⁵⁵, G. Safronov³⁷, G. Sajot¹⁴, A. Sánchez-Hernández³³, M.P. Sanders¹⁷, B. Sanghi⁵⁰, G. Savage⁵⁰, L. Sawyer⁶⁰, T. Scanlon⁴³, D. Schaile²⁵, R.D. Schamberger⁷², Y. Scheglov⁴⁰, H. Schellman⁵³, T. Schliephake²⁶, S. Schlobohm⁸², C. Schwanenberger⁴⁴, A. Schwartzman⁶⁸, R. Schwienhorst⁶⁵, J. Sekaric⁴⁹, H. Severini⁷⁵, E. Shabalina⁵¹, M. Shamim⁵⁹, V. Shary¹⁸, A.A. Shchukin³⁹, R.K. Shivpuri²⁸, V. Siccaldi¹⁹, V. Simak¹⁰, V. Sirotenko⁵⁰, P. Skubic⁷⁵, P. Slattery⁷¹, D. Smirnov⁵⁵, G.R. Snow⁶⁷, J. Snow⁷⁴, S. Snyder⁷³, S. Söldner-Rembold⁴⁴, L. Sonnenschein¹⁷, A. Sopczak⁴², M. Sosebee⁷⁸, K. Soustruznik⁹, B. Spurlock⁷⁸, J. Stark¹⁴, J. Steele⁶⁰, V. Stolin³⁷, D.A. Stoyanova³⁹, J. Strandberg⁶⁴, S. Strandberg⁴¹, M.A. Strang⁶⁹, E. Strauss⁷², M. Strauss⁷⁵, R. Ströhmer²⁵, D. Strom⁵³, L. Stutte⁵⁰, S. Sumowidagdo⁴⁹, P. Svoisky⁵⁵, A. Sznajder³, P. Tamburello⁴⁵, A. Tanasijczuk¹, W. Taylor⁶, B. Tiller²⁵, F. Tissandier¹³, M. Titov¹⁸, V.V. Tokmenin³⁶, I. Torchiani²³, D. Tsybychev⁷², B. Tuchming¹⁸, C. Tully⁶⁸, P.M. Tuts⁷⁰, R. Unalan⁶⁵, L. Uvarov⁴⁰, S. Uvarov⁴⁰, S. Uzunyan⁵², B. Vachon⁶, P.J. van den Berg³⁴, R. Van Kooten⁵⁴, W.M. van Leeuwen³⁴, N. Varelas⁵¹, E.W. Varnes⁴⁵, I.A. Vasilyev³⁹, M. Vaupel²⁶, P. Verdier²⁰, L.S. Vertogradov³⁶, M. Verzocchi⁵⁰, D. Vilanova¹⁸, F. Villeneuve-Seguier⁴³, P. Vint⁴³, P. Vokac¹⁰, E. Von Toerne⁵⁹, M. Voutilainen^{68,e}, R. Wagner⁶⁸, H.D. Wahl⁴⁹, L. Wang⁶¹, M.H.L.S. Wang⁵⁰, J. Warchol⁵⁵, G. Watts⁸², M. Wayne⁵⁵, G. Weber²⁴, M. Weber⁵⁰, L. Welty-Rieger⁵⁴, A. Wenger^{23,f}, N. Wermes²², M. Wetstein⁶¹, A. White⁷⁸, D. Wicke²⁶, G.W. Wilson⁵⁸, S.J. Wimpenny⁴⁸, M. Wobisch⁶⁰, D.R. Wood⁶³, T.R. Wyatt⁴⁴, Y. Xie⁷⁷, S. Yacoob⁵³, R. Yamada⁵⁰, W.-C. Yang⁴⁴, T. Yasuda⁵⁰, Y.A. Yatsunenko³⁶, H. Yin⁷, K. Yip⁷³, H.D. Yoo⁷⁷, S.W. Youn⁵³, J. Yu⁷⁸, C. Zeitnitz²⁶, S. Zelitch⁸¹, T. Zhao⁸², B. Zhou⁶⁴, J. Zhu⁷², M. Zielinski⁷¹, D. Ziemska⁵⁴, A. Zieminski^{54,‡}, L. Zivkovic⁷⁰, V. Zutshi⁵², and E.G. Zverev³⁸

(*The DØ Collaboration*)

¹Universidad de Buenos Aires, Buenos Aires, Argentina

²LAFEX, Centro Brasileiro de Pesquisas Físicas, Rio de Janeiro, Brazil

³Universidade do Estado do Rio de Janeiro, Rio de Janeiro, Brazil

⁴Universidade Federal do ABC, Santo André, Brazil

⁵Instituto de Física Teórica, Universidade Estadual Paulista, São Paulo, Brazil

⁶University of Alberta, Edmonton, Alberta, Canada,

Simon Fraser University, Burnaby, British Columbia,
Canada, York University, Toronto, Ontario, Canada,
and McGill University, Montreal, Quebec, Canada

⁷University of Science and Technology of China, Hefei, People's Republic of China

⁸Universidad de los Andes, Bogotá, Colombia

⁹Center for Particle Physics, Charles University, Prague, Czech Republic

¹⁰Czech Technical University, Prague, Czech Republic

¹¹Center for Particle Physics, Institute of Physics,

Academy of Sciences of the Czech Republic, Prague, Czech Republic

¹²Universidad San Francisco de Quito, Quito, Ecuador

¹³LPC, Université Blaise Pascal, CNRS/IN2P3, Clermont, France

¹⁴LPSC, Université Joseph Fourier Grenoble 1, CNRS/IN2P3,

Institut National Polytechnique de Grenoble, Grenoble, France

¹⁵CPPM, Aix-Marseille Université, CNRS/IN2P3, Marseille, France

¹⁶LAL, Université Paris-Sud, IN2P3/CNRS, Orsay, France

¹⁷LPNHE, IN2P3/CNRS, Universités Paris VI and VII, Paris, France

¹⁸CEA, Irfu, SPP, Saclay, France

¹⁹IPHC, Université Louis Pasteur, CNRS/IN2P3, Strasbourg, France

²⁰IPNL, Université Lyon 1, CNRS/IN2P3, Villeurbanne, France and Université de Lyon, Lyon, France

²¹III. Physikalisches Institut A, RWTH Aachen University, Aachen, Germany

²²Physikalisches Institut, Universität Bonn, Bonn, Germany

²³Physikalisches Institut, Universität Freiburg, Freiburg, Germany

²⁴Institut für Physik, Universität Mainz, Mainz, Germany

²⁵Ludwig-Maximilians-Universität München, München, Germany

²⁶Fachbereich Physik, University of Wuppertal, Wuppertal, Germany

²⁷Panjab University, Chandigarh, India

²⁸Delhi University, Delhi, India

²⁹Tata Institute of Fundamental Research, Mumbai, India

- ³⁰University College Dublin, Dublin, Ireland
³¹Korea Detector Laboratory, Korea University, Seoul, Korea
³²SungKyunKwan University, Suwon, Korea
³³CINVESTAV, Mexico City, Mexico
³⁴FOM-Institute NIKHEF and University of Amsterdam/NIKHEF, Amsterdam, The Netherlands
³⁵Radboud University Nijmegen/NIKHEF, Nijmegen, The Netherlands
³⁶Joint Institute for Nuclear Research, Dubna, Russia
³⁷Institute for Theoretical and Experimental Physics, Moscow, Russia
³⁸Moscow State University, Moscow, Russia
³⁹Institute for High Energy Physics, Protvino, Russia
⁴⁰Petersburg Nuclear Physics Institute, St. Petersburg, Russia
⁴¹Lund University, Lund, Sweden, Royal Institute of Technology and Stockholm University, Stockholm, Sweden, and Uppsala University, Uppsala, Sweden
⁴²Lancaster University, Lancaster, United Kingdom
⁴³Imperial College, London, United Kingdom
⁴⁴University of Manchester, Manchester, United Kingdom
⁴⁵University of Arizona, Tucson, Arizona 85721, USA
⁴⁶Lawrence Berkeley National Laboratory and University of California, Berkeley, California 94720, USA
⁴⁷California State University, Fresno, California 93740, USA
⁴⁸University of California, Riverside, California 92521, USA
⁴⁹Florida State University, Tallahassee, Florida 32306, USA
⁵⁰Fermi National Accelerator Laboratory, Batavia, Illinois 60510, USA
⁵¹University of Illinois at Chicago, Chicago, Illinois 60607, USA
⁵²Northern Illinois University, DeKalb, Illinois 60115, USA
⁵³Northwestern University, Evanston, Illinois 60208, USA
⁵⁴Indiana University, Bloomington, Indiana 47405, USA
⁵⁵University of Notre Dame, Notre Dame, Indiana 46556, USA
⁵⁶Purdue University Calumet, Hammond, Indiana 46323, USA
⁵⁷Iowa State University, Ames, Iowa 50011, USA
⁵⁸University of Kansas, Lawrence, Kansas 66045, USA
⁵⁹Kansas State University, Manhattan, Kansas 66506, USA
⁶⁰Louisiana Tech University, Ruston, Louisiana 71272, USA
⁶¹University of Maryland, College Park, Maryland 20742, USA
⁶²Boston University, Boston, Massachusetts 02215, USA
⁶³Northeastern University, Boston, Massachusetts 02115, USA
⁶⁴University of Michigan, Ann Arbor, Michigan 48109, USA
⁶⁵Michigan State University, East Lansing, Michigan 48824, USA
⁶⁶University of Mississippi, University, Mississippi 38677, USA
⁶⁷University of Nebraska, Lincoln, Nebraska 68588, USA
⁶⁸Princeton University, Princeton, New Jersey 08544, USA
⁶⁹State University of New York, Buffalo, New York 14260, USA
⁷⁰Columbia University, New York, New York 10027, USA
⁷¹University of Rochester, Rochester, New York 14627, USA
⁷²State University of New York, Stony Brook, New York 11794, USA
⁷³Brookhaven National Laboratory, Upton, New York 11973, USA
⁷⁴Langston University, Langston, Oklahoma 73050, USA
⁷⁵University of Oklahoma, Norman, Oklahoma 73019, USA
⁷⁶Oklahoma State University, Stillwater, Oklahoma 74078, USA
⁷⁷Brown University, Providence, Rhode Island 02912, USA
⁷⁸University of Texas, Arlington, Texas 76019, USA
⁷⁹Southern Methodist University, Dallas, Texas 75275, USA
⁸⁰Rice University, Houston, Texas 77005, USA
⁸¹University of Virginia, Charlottesville, Virginia 22901, USA and
⁸²University of Washington, Seattle, Washington 98195, USA

(Dated: September 16, 2008)

We measure the mass of the top quark using top quark pair candidate events in the lepton+jets channel from data corresponding to 1 fb^{-1} of integrated luminosity collected by the D0 experiment at the Fermilab Tevatron collider. We use a likelihood technique that reduces the jet energy scale uncertainty by combining an *in-situ* jet energy calibration with the independent constraint on the jet energy scale (JES) from the calibration derived using photon+jets and dijet samples. We find the mass of the top quark to be $171.5 \pm 1.8(\text{stat.+JES}) \pm 1.1(\text{syst.}) \text{ GeV}$.

Since the discovery of the top quark in 1995 [1], a substantial effort has gone into measuring and understanding its properties. Its large mass suggests a unique role in the mechanism of electroweak symmetry breaking. Through radiative corrections, a precise measurement of the top quark mass, together with that of the W boson, allows indirect constraints to be placed on the mass of the standard model Higgs boson [2]. A precise knowledge of the top quark mass could also provide a useful constraint to possible extensions of the standard model. It is therefore of great importance to continue improving measurements of the top quark mass [3, 4].

In this Letter, we present the most precise single measurement of the top quark mass from Run II of the Fermilab Tevatron collider. It uses a matrix element (ME) method with an *in-situ* jet energy calibration based on a global factor used to scale all jet energies and thereby the invariant mass of the hadronic W boson [3, 5]. This mass is constrained to the well known value of 80.4 GeV through the Breit-Wigner function for the hadronic W boson in the ME for $t\bar{t}$ production. The jet energy scale is further constrained to the standard scale derived from photon+jets and dijet samples within its uncertainties through the use of a prior probability distribution. This analysis is based on data collected by the D0 detector [6] from April 2002 to February 2006 comprising 1 fb^{-1} of integrated luminosity from $p\bar{p}$ collisions at $\sqrt{s} = 1.96 \text{ TeV}$.

The top quark is assumed to always decay into a W boson and a b quark producing a $W^+W^-b\bar{b}$ final state from $t\bar{t}$ production. This analysis is based on the lepton+jets channel with one W boson decaying via $W \rightarrow \ell\nu$ and the other via $W \rightarrow q\bar{q}'$. This channel is characterized by a lepton with large transverse momentum (p_T), large momentum imbalance due to the undetected neutrino (\not{p}_T), and four high- p_T jets. Events are selected for this analysis by requiring exactly one isolated electron (muon) with $p_T > 20 \text{ GeV}$ and $|\eta| < 1.1$ ($|\eta| < 2$), $\not{p}_T > 20 \text{ GeV}$, and exactly four jets with $p_T > 20 \text{ GeV}$ and $|\eta| < 2.5$, where the pseudorapidity $\eta = -\ln [\tan(\theta/2)]$, and θ is the polar angle with respect to the proton beam direction. Multijet background, typically originating from lepton or jet energy mismeasurements, is further suppressed by requiring the lepton direction and \not{p}_T vector to be separated in azimuth. Jets are reconstructed using a cone algorithm [7] with radius $R = \sqrt{(\Delta y)^2 + (\Delta\phi)^2} = 0.5$ where the y is the rapidity. Jet energies are corrected to the particle level using corrections derived from photon+jet and dijet samples. Jets containing a muon are assumed to originate from semileptonic b quark decays and corrected by the muon momentum and average neutrino energy. At least one jet is required to be tagged by a neural-network based algorithm [8] as a b -jet candidate. The tagging efficiency for b jets is $\sim 50\%$ with a misidentification rate of $\sim 1\%$ from light jets. A total of 220 events, split equally between the electron and muon channels, satisfying these criteria is selected.

The top quark mass is determined from the data sample with a likelihood method based on per-event probability densities (p.d.'s) constructed from the MEs of the processes contributing to the observed events. Assuming only two processes, $t\bar{t}$ and $W+\text{jets}$ production, the p.d. to observe an event with measured variables x is

$$P_{\text{evt}} = A(x) [f P_{\text{sig}}(x; m_t, k_{\text{jes}}) + (1 - f) P_{\text{bkg}}(x; k_{\text{jes}})],$$

where the top quark mass m_t , jet energy scale factor k_{jes} dividing the energies of all jets, and observed signal fraction f are the parameters to determine from data. P_{sig} and P_{bkg} are, respectively, p.d.'s for $t\bar{t}$ and $W+\text{jets}$ production. Multijet events satisfy $P_{\text{bkg}} \gg P_{\text{sig}}$ and are also represented by P_{bkg} . $A(x)$ is a function only of x and accounts for the geometrical acceptance and efficiencies.

P_{sig} and P_{bkg} are calculated by integrating over all possible parton states leading to the measured set x . In addition to the partonic final state described by the variables y , these states include the initial state partons carrying momenta q_1 and q_2 in the colliding p and \bar{p} . The integration involves a convolution of the partonic differential cross section $d\sigma(y; m_t)$ with the p.d.'s for the initial state partons $f(q_i)$ and the transfer function $W(y, x; k_{\text{jes}})$:

$$P_{\text{sig}} = \frac{1}{N} \int \sum d\sigma(y; m_t) dq_1 dq_2 f(q_1) f(q_2) W(y, x; k_{\text{jes}}),$$

where the sum runs over all possible initial state parton flavor combinations. $f(q_i)$ includes parton density functions (PDFs) for finding a parton of a given flavor and longitudinal momentum fraction in the p or \bar{p} (CTEQ6L1 [9]) and parameterizations of the p.d.'s for the transverse components of q_i derived from PYTHIA [10]. Jet fragmentation effects and experimental resolution are taken into account by $W(y, x; k_{\text{jes}})$, representing the p.d. for the measured set x to have arisen from the partonic set y . The normalization factor N , defined as the expected observed cross section for a given (m_t, k_{jes}) , ensures $A(x)P_{\text{sig}}$ (and ultimately P_{evt}) is normalized to unity.

The differential cross section term in P_{sig} is calculated using the leading order ME for $q\bar{q} \rightarrow t\bar{t}$. After all energy and momentum constraints are taken into account, this term is integrated over the energy associated with one of the quarks from the hadronic W boson decay, the masses of the two W bosons and two top quarks, and the energy ($1/p_T$) of the electron (muon). It is summed over 24 possible jet-parton assignments each carrying a b -jet tagging weight [11] and over the neutrino solutions. $W(y, x; k_{\text{jes}})$ is the product of five terms for the four jets and one charged lepton. The jet terms are parameterized in terms of jet energy with a function involving the sum of two Gaussians whose parameters depend linearly on parton energy. The term for the charged lepton is parameterized as a Gaussian distribution in energy ($1/p_T$) for electrons (muons). All

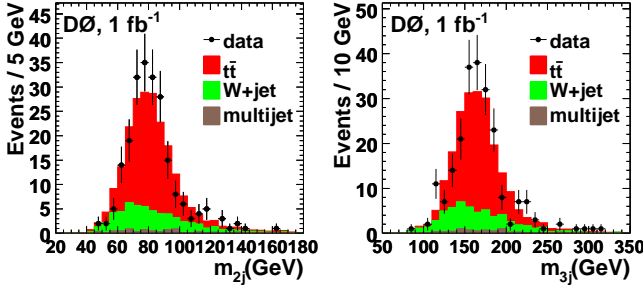


FIG. 1: Comparison between data and MC 2-jet (m_{2j}) and 3-jet (m_{3j}) invariant mass distributions.

parameters for $W(y, x; k_{\text{jes}})$ are derived using fully simulated Monte Carlo (MC) events. The normalization cross section $\sigma_{\text{obs}}^{t\bar{t}} = \int A(x)P_{\text{sig}}dx = \sigma^{t\bar{t}}(m_t)\langle A(m_t, k_{\text{jes}}) \rangle$ is calculated using the total cross section corresponding to the ME used and the mean acceptance for events whose dependencies on m_t and k_{jes} are determined from MC events.

The differential cross section term in P_{bkg} is calculated using the $W+4$ jets MEs provided by VECBOS [12]. The integration is performed over the energies of the four partons producing the jets, the W boson mass, and the energy ($1/p_T$) of the electron (muon) summing over 24 possible jet-parton assignments and two neutrino solutions. The transverse momenta of the initial state partons are assumed to be zero.

P_{sig} and P_{bkg} are calculated using MC techniques on a grid in (m_t, k_{jes}) having spacings of 1.5 GeV and 0.015, respectively. At each grid point, a likelihood function, $L(x; m_t, k_{\text{jes}}, f)$, is constructed from the product of the individual event p.d.'s (P_{evt}) and f is determined by minimizing $-\ln L$ at that point. $L(x; m_t, k_{\text{jes}})$ is then projected onto the m_t and k_{jes} axes according to $L(x; m_t) = \int L(x; m_t, k_{\text{jes}})G(k_{\text{jes}})dk_{\text{jes}}$ and $L(x; k_{\text{jes}}) = \int L(x; m_t, k_{\text{jes}})dm_t$. The prior $G(k_{\text{jes}})$ is a Gaussian function centered at $k_{\text{jes}} = 1$ with width $\sigma = 0.019$ determined from the photon+jets and dijet samples used in the standard jet energy scale calibration. Best estimates of m_t and k_{jes} and their uncertainties are then extracted from the mean and rms of $L(x; m_t)$ and $L(x; k_{\text{jes}})$.

The measurement technique described above is calibrated using MC events produced with the ALPGEN event generator [13] employing PYTHIA for parton showering and hadronization and implementing the MLM matching scheme [14]. All generated events are processed by a full GEANT [15] detector simulation followed by the same reconstruction and analysis programs used on data. Fig. 1 shows comparisons of the 2-jet and 3-jet invariant mass distributions between data and MC using $t\bar{t}$ events with a true top quark mass (m_t^{true}) of 170 GeV. These are calculated using jets assigned as the decay products of the top quark and W boson from the hadronic branch

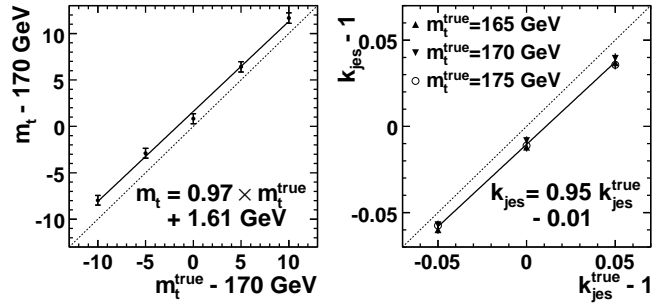


FIG. 2: Mean values of m_t and k_{jes} from ensemble tests versus true values parameterized by straight lines. Dashed lines represent identical fitted and true values.

in the permutation with the largest weight (defined as the product of P_{sig} and the b -jet tagging weight) around the peak of $L(x; m_t, k_{\text{jes}})$. MC distributions are normalized to data distributions with $f = 0.74$ determined from data. The background includes simulated $W+\text{jets}$ events and data events selected from a multijet enriched sample. The latter comprises 12% of the total background based on estimates from data. The estimated number of $t\bar{t}$ events ($e + \text{jets}$: 91 ± 9 , $\mu + \text{jets}$: 71 ± 8) agrees with the expectation ($e + \text{jets}$: 89 ± 6 , $\mu + \text{jets}$: 73 ± 5).

Five $t\bar{t}$ MC samples are generated with $m_t^{\text{true}} = 160$, 165, 170, 175, and 180 GeV, with six more produced from three of these by scaling all jet energies by $\pm 5\%$. P_{sig} and P_{bkg} are calculated for these events from which pseudo-experiments fixed to the number of data events are randomly drawn with a signal fraction fluctuated according to a binomial distribution around that determined from data. The mean values of m_t and k_{jes} for 1000 pseudo-experiments are shown in Fig. 2 as functions of the true values and fitted to a straight line. The average widths of the m_t and k_{jes} pull distributions are 1.0 and 1.1, respectively. The pull is defined as the deviation of a measurement from the mean of all measurements divided by the uncertainty of the measurement per pseudo-experiment. The measured uncertainties in data are corrected by the deviation of the average pull width from 1.0.

$L(x; m_t)$ and $L(x; k_{\text{jes}})$ for the selected data samples are calibrated according to the parameterizations shown in Fig. 2. $L(x; m_t)$ is shown in Fig. 3(a) with a measured $m_t = 171.5 \pm 1.8(\text{stat.+JES})$ GeV. The measured $k_{\text{jes}} = 1.030 \pm 0.017$ represents a 1.2σ shift from $k_{\text{jes}} = 1$ where σ is the sum in quadrature of the width of $G(k_{\text{jes}})$ and the uncertainty of the measured k_{jes} . Fig. 3(b) compares the measured uncertainty for m_t with the expected uncertainty distribution from pseudo-experiments in MC assuming $m_t^{\text{true}} = 170$ GeV.

To verify the *in-situ* jet energy calibration, we repeat the analysis on data by fixing k_{jes} to the measured value and removing the W boson mass constraint, replacing $L(x; m_t, k_{\text{jes}}, f)$ with $L(x; m_t, m_W, f)$. P_{sig} and P_{bkg} are

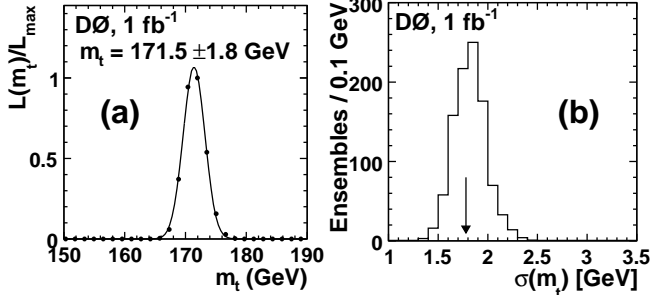


FIG. 3: (a) Projection of data likelihood onto the m_t axis with best estimate shown. (b) Expected uncertainty distribution for m_t with measured uncertainty indicated by the arrow.

TABLE I: Summary of systematic uncertainties (symmetrized based on the larger of the two values in each direction).

Source	Uncertainty (GeV)
<i>Physics modeling:</i>	
Signal modeling	± 0.40
PDF uncertainty	± 0.14
Background modeling	± 0.10
b -fragmentation	± 0.03
<i>Detector Modeling:</i>	
b /light response ratio	± 0.83
Jet identification and resolution	± 0.26
Trigger	± 0.19
Residual jet energy scale	± 0.10
Muon resolution	± 0.10
<i>Method:</i>	
MC calibration	± 0.26
b -tagging efficiency	± 0.15
Multijet contamination	± 0.14
Signal contamination	± 0.13
Signal fraction	± 0.09
Total	± 1.07

now calculated on a grid in (m_t, m_W) having spacings of 1.5 GeV and 1 GeV, respectively. $L(x; m_t)$ and $L(x; m_W)$ are calculated in the same way as for the grid in (m_t, k_{jes}) except that no prior probability distribution is used for $L(x; m_t)$. We find $m_W = 80.3 \pm 1.0$ GeV which is consistent with the constraint of 80.4 GeV.

Systematic uncertainties are evaluated for three categories. The first category involves the modeling of MC $t\bar{t}$ and W +jets events and includes uncertainties in the modeling of extra jets due to radiation in $t\bar{t}$ events, the distribution shapes and the heavy flavor fraction in W +jets events, b fragmentation, and the PDFs used in generating events. The second category is associated with the simulation of detector response and includes possible effects due to the energy and $|\eta|$ dependence of the jet energy scale unaccounted for by the *in-situ* calibration, uncertainties in the modeling of the relative calorimeter response to b and light quark jets, and uncertainties associated with the simulation of jet energy

resolution and reconstruction efficiency, muon p_T resolution, and trigger efficiency. The third category is related to assumptions made in the method and uncertainties in the calibration and includes possible effects due to the exclusion of multijet events and non-lepton+jets $t\bar{t}$ events from the calibration procedure, uncertainties in the signal fraction used in ensemble tests, and uncertainties associated with the parameters defining the calibration curve. Contributions from all these sources are summarized in Table I and sum in quadrature to ± 1.1 GeV.

The leading sources of uncertainty in Table I are those associated with the b /light response ratio and signal modeling. The first of these is evaluated by estimating the possible difference in this ratio between data and MC and scaling the energies of all jets matched to b quarks in a MC $t\bar{t}$ sample by this amount. The analysis is repeated for this sample and the difference in m_t from that of the unscaled sample taken as the uncertainty. The uncertainty associated with the modeling of additional jets in $t\bar{t}$ events is evaluated using both data and MC samples. Using MC $t\bar{t}$ events, the fraction of $t\bar{t}$ signal events with ≥ 5 jets is varied such that the ratio of 4-jet to ≥ 5 -jet events in MC matches that in data including its uncertainties. The difference in the resulting m_t from that of the default sample is taken as the uncertainty. Using data, this is done through ensemble tests in which a fixed number of ≥ 5 -jet events not used in the measurement are randomly drawn for each experiment and combined with the default sample of 4-jet events. The ensemble tests are repeated for different fractions of ≥ 5 -jet events constituting up to 30% of each experiment. m_t for the default sample is compared with the mean from each ensemble test and the largest difference taken as the systematic uncertainty. Both procedures yield consistent estimates for this systematic uncertainty.

In summary, we present a measurement of the top quark mass using $t\bar{t}$ lepton+jets events from 1 fb^{-1} of data collected by the D0 experiment. Using a ME technique combining an *in-situ* calibration of the jet energy scale with the calibration based on the photon+jets and dijet samples gives us

$$m_t = 171.5 \pm 1.8(\text{stat.+JES}) \pm 1.1(\text{syst.}) \text{ GeV},$$

representing the most precise single measurement to date.

We thank the staffs at Fermilab and collaborating institutions, and acknowledge support from the DOE and NSF (USA); CEA and CNRS/IN2P3 (France); FASI, Rosatom and RFBR (Russia); CNPq, FAPERJ, FAPESP and FUNDUNESP (Brazil); DAE and DST (India); Colciencias (Colombia); CONACyT (Mexico); KRF and KOSEF (Korea); CONICET and UBACyT (Argentina); FOM (The Netherlands); STFC (United Kingdom); MSMT and GACR (Czech Republic); CRC Program, CFI, NSERC and WestGrid Project (Canada); BMBF and DFG (Germany); SFI (Ireland); The Swedish Research Council (Sweden); CAS and CNSF (China);

and the Alexander von Humboldt Foundation (Germany).

- [a] Visitor from Augustana College, Sioux Falls, SD, USA.
- [b] Visitor from The University of Liverpool, Liverpool, UK.
- [c] Visitor from ECFM, Universidad Autonoma de Sinaloa, Culiacán, Mexico.
- [d] Visitor from II. Physikalisches Institut, Georg-August University, Göttingen, Germany.
- [e] Visitor from Helsinki Institute of Physics, Helsinki, Finland.
- [f] Visitor from Universität Zürich, Zürich, Switzerland.
- [‡] Deceased.

- [1] F. Abe *et al.* (CDF Collaboration), Phys. Rev. Lett. **74**, 2626 (1995); S. Abachi *et al.* (D0 Collaboration), Phys. Rev. Lett. **74**, 2632 (1995).
- [2] Tevatron Electroweak Working Group, <http://tevewwg.fnal.gov>.
- [3] V. Abazov *et al.* (D0 Collaboration), Phys. Rev. D **74**, 092005 (2006).

- [4] T. Aaltonen *et al.* (CDF Collaboration), Phys. Rev. Lett. **99**, 182002 (2007).
- [5] V. Abazov *et al.* (D0 Collaboration), Nature **429**, 638 (2004).
- [6] V. Abazov *et al.* (D0 Collaboration), Nucl. Instrum. Methods Phys. Res. Sect. A **565**, 463 (2006).
- [7] G.C. Blazey *et al.*, arXiv:hep-ex/0005012 (2000).
- [8] T. Scanlon, Ph.D. thesis, FERMILAB-THESIS-2006-43.
- [9] J. Pumplin *et al.*, JHEP **0207**, 012 (2002).
- [10] T. Sjöstrand *et al.*, Comp. Phys. Commun. **135**, 238 (2001).
- [11] The weight for a b -tagged jet with a given p_T and η under a parton flavor hypothesis $\alpha (= b, c, \text{light } q \text{ or gluon})$ is given by the parameterization of the average tagging efficiency $\epsilon_\alpha(p_T, \eta)$. Consequently, the weight for a jet not b -tagged is $1 - \epsilon_\alpha(p_T, \eta)$. The event weight is defined as the product of jet weights.
- [12] F.A. Berends *et al.*, Nucl. Phys. **B357**, 32 (1991).
- [13] M.L. Mangano *et al.*, JHEP **307**, 001 (2003).
- [14] S. Höche *et al.*, arXiv:hep-ph/0602031 (2006).
- [15] R. Brun and F. Carminati, CERN Program Library Long Writeup W5013, 1993 (unpublished).